Glycobiology vol. 23 no. 1 pp. 106–120, 2013
doi:10.1093/glycob/cws134
Advance Access publication on September 20, 2012

Toxoplasma gondii secretory proteins bind to sulfated heparin structures

Nahid Azzouz[2], Faustin Kamena[3], Paola Laurino[2], Raghavendra Kikkeri[2,4], Corinne Mercier[5], Marie-France Cesbron-Delauw[5], Jean-François Dubremetz[6], Luisa De Cola[7], and Peter H Seeberger[1,2]

[2]Department of Biomolecular Systems, the Freie Universität Berlin, Max-Planck-Institute of Colloids and Interfaces, Am Mühlenberg 1, 14476 Potsdam, Germany; [3]Max-Planck-Institute for Infection Biology, Berlin, Germany; [4]Indian Institute of Science Education and Research (IISER) First floor, Pashan Pune, Maharashtra 411021, India; [5]Laboratoire Adaptation et Pathogénie des Micro-Organismes, CNRS UMR 5163, Université Joseph Fourier, Grenoble, France; [6]CNRS UMR 5539, Université Montpellier II, Montpellier, France; and [7]Physikalisches Institut and Center for Nanotechnology of Westfälische Wilhelms-Universität, Münster, Germany

Received on April 10, 2012; revised on September 15, 2012; accepted on September 15, 2012

***Toxoplasma gondii* is the causative agent of toxoplasmosis, one of the most widespread infections in humans and animals, and is a major opportunistic pathogen in immunocompromised patients. *Toxoplasma gondii* is unique as it can invade virtually any nucleated cell, although the mechanisms are not completely understood. Parasite attachment to the host cell is a prerequisite for reorientation and penetration and likely requires the recognition of molecules at the host cell surface. It has been reported that the affinity of tachyzoites, the invasive form of *T. gondii*, for host cells can be inhibited by a variety of soluble-sulfated glycosaminoglycans (GAGs), such as heparan sulfate. Using heparin-functionalized zeolites in the absence of host cells, we visualized heparin-binding sites on the surface of tachyzoites by confocal and atomic force microscopy. Furthermore, we report that protein components of the parasite rhoptry, dense granule and surface bind GAGs. In particular, the proteins ROP2 and ROP4 from the rhoptry, GRA2 from the dense granules and the surface protein SAG1 were found to bind heparin. The binding specificities and affinities of individual parasite proteins for natural heparin and heparin oligosaccharides were determined by a combination of heparin oligosaccharide microarrays and surface plasmon resonance. Our results suggest that interactions between sulfated GAGs and parasite surface antigens contribute to *T. gondii* attachment to host cell surfaces as well as initiating the invasion process, while rhoptries and dense granule organelles may play an important role during the establishment of the infection and during the life of the parasite inside the parasitophorous vacuole.**

Keywords: cell invasion / glycosaminoglycans / heparin-binding proteins / *Toxoplasma gondii*

Introduction

The phylum of Apicomplexa parasites which include both *Toxoplasma gondii* and *Plasmodium* spp. represents a particularly important class of pathogens because they can infect a broad range of eukaryotic host cells. For Apicomplexa, a prerequisite for invasion is the attachment of the parasite to the host cell, as well as reorientation prior to entering the host, steps that are mediated by both parasite and host cell surface molecules (Mineo et al. 1993; Jacquet et al. 2001). Considering that *T. gondii* can infect a wide variety of nucleated cells and that *T. gondii* mutants deficient in surface proteins such as SAG1 can still infect host cells (Lekutis et al. 2001; Brenier-Pinchart et al. 2006), parasites must be able to access multiple adhesion molecules and overlapping pathways to invade cells (Soldati et al. 2004). However, because these parasites can utilize multiple redundant invasion pathways, it has been difficult to assess the relative contribution of individual binding events to the infection process.

Apicomplexan parasites possess complex molecular machinery, comprised of both intracellular as well as extracellular components, that powers gliding motility and host cell invasion and has been well described elsewhere (Soldati et al. 2004; Cowman and Crabb 2006). In addition to gliding motility and adhesion, successful host cell invasion requires that secretory organelles, including micronemes and rhoptries, are integrated into the apical complex during a preliminary phase of the infection (Dubremetz et al. 1998; Carruthers and Sibley 1999; Black and Boothroyd 2000; Soldati et al. 2001). During host cell entry, the contents of the micronemes, rhoptries and dense granules are sequentially released (Carruthers and Sibley 1997). All these events lead to the creation of the parasitophorous vacuole within the host cell, in which parasites undergo rapid multiplication (Carruthers and Boothroyd 2007; Plattner and Soldati-Favre 2008; Soldati-Favre 2008; Blader and Saeij 2009). Microneme proteins and their proteolytic trimming fragments are considered to be a major class of cellular adhesins involved in recognition and attachment to host

[1]To whom correspondence should be addressed: Tel: +49-30-838-59300; Fax: +49-30-838-59302; e-mail: peter.seeberger@mpikg.mpg.de

cells (Carruthers and Sibley 1999; Cérède et al. 2002; Barragan et al. 2005; Carruthers and Tomley 2008; El Hajj et al. 2008; Soldati-Favre 2008).

To understand and ultimately prevent host cell invasion by parasites, the earliest stages of infection, host cell recognition and attachment, must be defined. The most extensively investigated parasite-binding structures resident on the host cell surface are the proteoglycans and glycolipids, which have well-characterized roles in both cell signaling and cell–cell recognition (Varki 1997, 2008). However, during infection, both the pathogen and the host cell exploit these surface glycans for their own benefit. Pathogens interact with these molecules to initiate the infection process while, in host cells, particular glycan–protein interactions induce the transmission of intracellular alarm signals. A complex set of glycan-binding molecules have been shown to be expressed by apicomplexan pathogens (Boulanger et al. 2010).

To date, two major host cell surface ligands have been reported to be involved in the early steps of the Apicomplexa invasion process: sialic acid and glycosaminoglycans (GAGs). Sialic acid-dependent invasion is now unanimously accepted as the primary mechanism for infection by *Plasmodium falciparum* (Thompson et al. 2001; Baum et al. 2003; Triglia et al. 2005; Persson et al. 2008) and also *T. gondii* (Monteiro et al. 1998; Blumenschein et al. 2007; Garnett et al. 2009; Friedrich, Santos, et al. 2010), and some of the participating parasite and host cell surface molecules have been identified (Brown and Higgins 2010; Friedrich, Matthews, et al. 2010). GAG-dependent invasion is mediated by sulfated proteoglycans in particular in *P. falciparum* (Vogt et al. 2003; Coppi et al. 2007; Muthusamy et al. 2007; Achur et al. 2008; Boyle et al. 2010), and evidence of a role for host cell surface-sulfated GAGs in host cell recognition and attachment during the life cycle of *T. gondii* has been reported (Ortega-Barria and Boothroyd 1999; Carruthers et al. 2000; He et al. 2002). The importance of proteoglycans for successful invasion of host cells by *T. gondii* was first shown indirectly when various GAGs were shown to be effective inhibitors of the process (Ortega-Barria and Boothroyd 1999). For example, free heparin, fucoidan or dextran sulfate were able to bind to the surface of tachyzoites and prevent the parasite from invading human fibroblasts. However, the interaction has not been investigated at the molecular level to determine which parasite lectins are involved. The localization of FITC-labeled heparin to a site near the subapical region of extracellular tachyzoites provided additional evidence for parasite-associated lectins (Botero-Kleiven et al. 2001).

To identify the *T. gondii* carbohydrate-binding proteins that may participate in host cell recognition, we first determined whether host cell proteoglycans might mediate *T. gondii* attachment. GAG-binding proteins were isolated from the parasite cell surface and from its specialized secretory organelles. The glycan–protein binding specificities and kinetics were evaluated by synthetic glycan microarray and surface plasmon resonance (SPR). The *T. gondii* rhoptry proteins, ROP2 and ROP4, the dense granule protein GRA2 and the surface protein SAG1 were shown to be lectins that recognize the sulfated GAG polysaccharides, suggesting that these proteins are important for host cell invasion. Further structural analyses of these key parasite lectins are needed to reveal glycan-binding motifs and a glycan–protein interface that could be targeted by rationally designed drugs to block the early step of *T. gondii* invasion and prevent toxoplasmosis.

Results

Cell surface localization of heparin-binding proteins

To demonstrate that there are in fact GAG-binding proteins on the cell surface of *T. gondii*, *in situ* localization assays were performed. A heparin-functionalized neutral zeolite, a microporous, aluminosilicate mineral ligand, was assembled. To enable direct visualization by confocal microscopy, the heparin-functionalized zeolite was labeled with fluorescent Rhodamine (Figure 1A). The heparin-functionalized zeolite was incubated with purified *T. gondii* RH-88 strain expressing GRA1-green fluorescent protein (GFP) enabling simple visualization of the tachyzoites, while avoiding the need for antibodies that could interfere with or produce an artifact in the binding assays. A heparin-free but otherwise identically functionalized zeolite polymer was used as a control. A volume equivalent to 1×10^8 parasites were suspended in phosphate-buffered saline (PBS) buffer and incubated with either the heparin-functionalized or the control zeolite. Parasites were then washed with PBS buffer to remove unbound zeolite and then fixed and prepared for confocal microscopy. Incubation of tachyzoites with the heparin-functionalized particles resulted in decoration of the parasite cell surface with red clusters of rhodamine-labeled zeolite (Figure 1C and D). Incubation of tachyzoites with the control, heparin-free zeolite did not result in surface labeling (Figure 1B), strongly indicating that this effect is a result of interactions between heparin and heparin-binding cell surface molecules. Finally, high-resolution atomic force microscopy (AFM) was employed to confirm the presence of bound heparin-functionalized zeolite at the parasite cell surface. The surface topology of a single tachyzoite after incubation with the heparin-functionalized polymer revealed the presence of the polymer (black arrows) on the parasite surface (Figure 1E). Together, confocal microscopy and AFM data allowed for the visualization of the heparin-binding sites on the surface of individual tachyzoites in the absence of host cells. Our results show that tachyzoites are primed to bind sulfate proteoglycans and that this interaction occurs during their initial contact with host cells.

An interaction between host cells sulfated GAGs and T. gondii proteins

To show the importance of *T. gondii* protein–host cell surface sulfated proteoglycans binding during the infection of Vero (African Green Monkey Kidney) cells, we developed an infection assay using purified, metabolically labeled tachyzoites. When incubated with a monolayer of Vero cells, [^{3}H] glucosamine-labeled tachyzoites successfully attached to and invaded the cells. The degree of infection was evaluated by counting the level of radioactivity that remained after extensively washing the cells to remove parasites that were not tightly attached to the monolayer. Deaminated 5 kDa natural heparin, chondroitin sulfate (CS)-A, CS-B (dermatan sulfate), hyposulfated (hypoS) fucoidans from alga *Fucus evanescens*

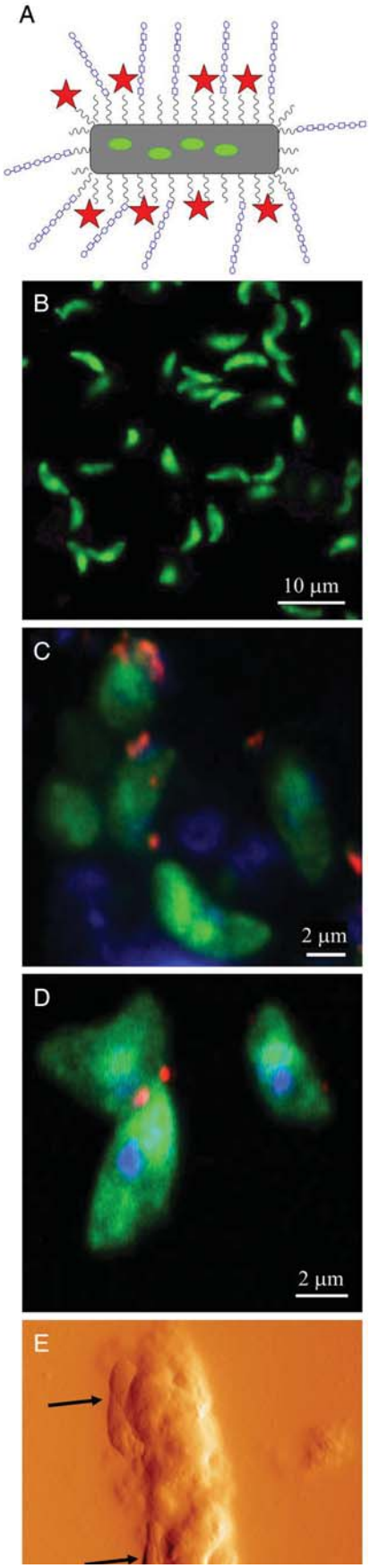

and synthetic trimannose oligosaccharide were used as competitive inhibitors to block infection. Figure 2 shows that heparin had the strongest inhibitory effect which resulted in a decreased radioactivity of the Vero cell monolayer post-infection, indicating that the presence of heparin in solution strongly reduced the ability of tachyzoites to infect Vero cell monolayers (Figure 2A). The ability of free heparin to inhibit infection suggests the involvement of host cell surface GAG structures in the infection process. When purified, labeled tachyzoites were preincubated with 10 µg/mL of heparin, 90% inhibition was reached (Figure 2A). At heparin concentrations of 20 µg/mL and above, no further significant decrease in the amount of measured radioactivity was observed (data not shown). This observation indicates that it may be possible to saturate the accessible lectins on the surface of the parasite and that parasites may be able to simultaneously access multiple invasion pathways during infection of host cells. As already reported in the case of *T. gondii* grown in human foreskin fibroblast cells (Ortega-Barria and Boothroyd 1999), we found that the infectivity of Vero cells was not inhibited by CS-A and CS-B except at very high concentrations (Figure 2A). As a control, we tested the ability of non-sulfated synthetic trimannose oligosaccharide to inhibit invasion. Figure 2A shows that this oligosaccharide failed to inhibit attachment/invasion even up to 10 mg/mL, which is 100-fold higher than the concentration of heparin that resulted in maximum inhibition. Furthermore, the hypoS fucoidan polysaccharide showed binding inhibition only at higher concentration (10 mg/mL), suggesting that the sulfation of the polysaccharide is critical for lectin–oligosaccharide interaction to occur. To further investigate whether the degree of GAG sulfation influences lectin recognition and binding, we incubated the Vero cells with sodium chlorate ($NaClO_3$). $NaClO_3$ is an inhibitor of proteoglycan sulfation (Humphries and Silbert 1988) which was previously shown to have no effect on protein synthesis and no toxic effects on cells (Baeuerle and Huttner 1986). Preincubation of Vero cell monolayers in the presence of various concentrations of $NaClO_3$ prior to parasite infection reduced the level of monolayer-associated radioactivity resulting from tachyzoite binding by 50% at 20 mM and by 70% at 50 mM (Figure 2C). The results obtained in the case of Vero cells infected with sag1 knockout (KO) mutant (Figure 2B) showed a decrease of 10% inhibition in the presence of heparin compared with wild type (wt) strain, suggesting a role of SAG1 in adhesion/invasion. The binding of heparin to *T. gondii* tachyzoites prepared from wt strain and from SAG1 and GRA2 deletion mutants was further investigated by flow cytometry to enable a quantitative binding of heparin-functionalized zeolite. The measurements showed a similar binding for both wt RH (Sabin 1941) and

Fig. 1. Confocal microscopy and AFM images of the *T. gondii*–heparin interaction. (**A**) Design of the zeolite functionalized with heparin. (**B**) Tachyzoites incubated with non-functionalized zeolite. (**C** and **D**) Confocal laser scanning microscopy images of *T. gondii* purified tachyzoites incubated with zeolite functionalized with heparin. (**E**) The AFM image of a single tachyzoite incubated with zeolite functionalized with heparin. The zeolite is indicated by black arrows. Heparin, blue; DXP (*N*,*N*′-*bis*(2,6-dimethylphenyl) perylene 3,4,9,10-tertracarboxylic diimide), green; rhodamine, red; linker, black.

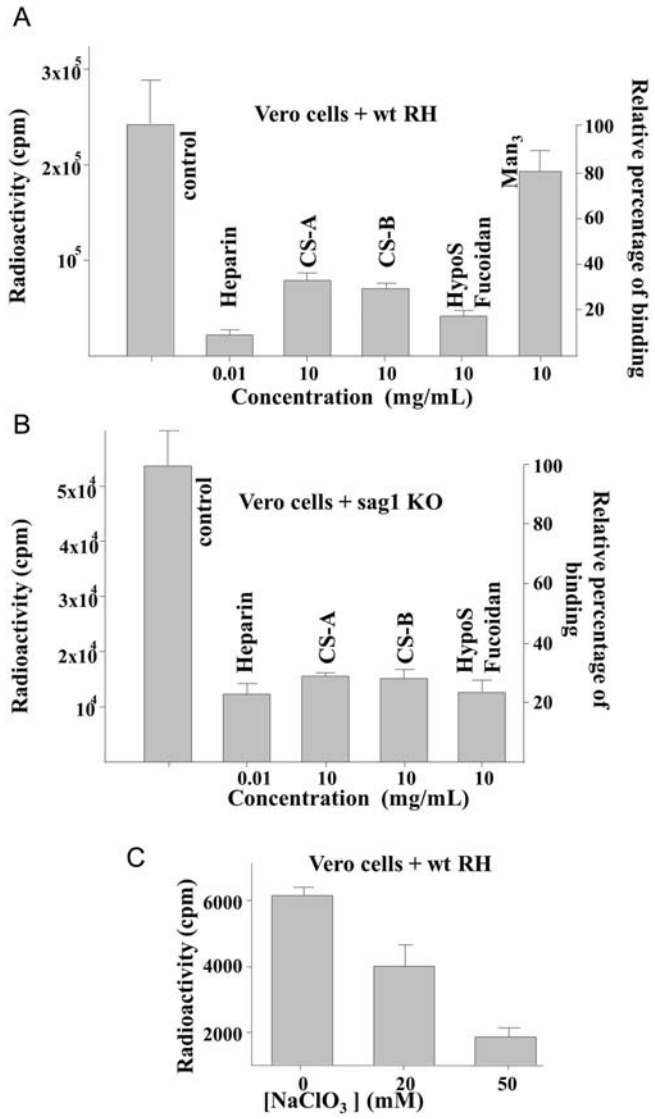

Fig. 2. Effect of polysaccharides and inhibitor of proteoglycan sulfation during *T. gondii* infection of Vero cells. (**A**) Vero cells infected with [^{3}H] glucosamine labeled wt RH tachyzoites in the presence of heparin, CS-A, CS-B, hypoS fucoidans from alga *F. evanescens* or synthetic trimannose oligosaccharide. (**B**) Vero cells infected with [^{3}H]glucosamine-labeled sag1 KO RH tachyzoites in the presence of heparin, CS-A, CS-B or hypoS fucoidans from alga *F. evanescens*. (**C**) Vero cells were treated for 12 h with $NaClO_3$ at the indicated concentrations prior to infection with [^{3}H] glucosamine-labeled wt RH tachyzoites. After washing of cell monolayers, the number of labeled tachyzoites remaining was determined by counting the emitted radiations. Results are given as the mean of two experiments.

GRA2 deletion mutant (Figure 3B and D). In contrast, the binding is around 30% lower in the case of the SAG1 deletion mutant (Figure 3F), confirming the decrease of 10% inhibition observed in attachment/invasion assays (Figure 2B). The large population in the control of delta SAG1 is due to non-viable cells that become auto-fluorescent.

Although the growth of the SAG1 mutant is very slow, the fact that the SAG1 mutant is still able to infect host cells in the presence of heparin support the hypothesis for additional cell surface GAG-binding proteins (Lekutis et al. 2001; Brenier-Pinchart et al. 2006) but also for non-GAG-binding pathways. Together, these data suggest that cell surface GAGs are involved in the early steps of attachment and the invasion of Vero cells by *T. gondii* tachyzoites and furthermore that the sulfate groups of GAGs are critical for the binding interactions.

Identification of T. gondii heparin-binding proteins

Using a heparin–agarose column, and an unconjugated agarose column as a control, we isolated *T. gondii* proteins that have an affinity for heparin. A total cell lysate was made from purified tachyzoites, and aliquots corresponding to 100 µg protein were loaded onto both the heparin-affinity chromatography column and the control column. Two fractions were collected from each column, one eluted with a low salt concentration wash (0.05 M NaCl) and another eluted with a higher salt concentration wash (0.2 M NaCl). Aliquots from each fraction were resolved by sodium dodecyl sulfate–polyacrylamide gel electrophoresis (SDS–PAGE) and proteins were detected by Coomassie staining. Using the unconjugated agarose column, no protein was isolated from the tachyzoite, extract under either 0.05 and 0.2 M NaCl salt conditions (Figure 4A, top panel). In contrast, four proteins were eluted from the heparin affinity column with 0.2 M NaCl, as shown by Coomassie-stained SDS–PAGE (Figure 4A, bottom panel, lane 2). The proteins, with molecular masses of 28, 36, 60 and 65 kDa (labeled 1–4), were eluted and identified by peptide mass fingerprinting after trypsin digestion. The most intense Coomassie-stained bands, 1 and 2, were identified as protein components of the rhoptry organelles and consist of a mixture of ROP2, ROP4 and ROP5 proteins. Band 3 was identified as the glycosylphosphatidylinositol-anchored surface protein SAG1, and band 4 as the dense granule protein GRA2. SAG3 protein reported to bind to heparin (Jacquet et al. 2001) was not identified, suggesting a need of an elution buffer with much higher salt concentration. The protein bands eluted at low salt concentration with molecular masses between 35 and 45 kDa were not identified due to their low affinity to heparin (Figure 4A, bottom panel, lane 1). To further confirm the identities of the eluted proteins, immunoblot analyses were performed with the same fractions of column eluate as used in Figure 4A, using either a monoclonal antibody (mAb) that specifically recognizes the protein GRA2, an mAb that recognizes both the ROP2 and ROP4 proteins (collectively referred to as ROP proteins) or an mAb that recognizes the protein SAG1. Due to column overloading part of the injected protein extract does not bind and eluted in the flow-through fraction including rhoptry (ROP) and granule (GRA) proteins. The immunoblots showed that the ROP proteins, GRA2 and SAG1 are indeed present in the 0.2 M NaCl eluate, confirming that these proteins have affinity for heparin and remain tightly bound during the 0.05 M salt wash and being eluted only under 0.2 M salt concentration (Figure 4B).

To confirm the binding of ROP proteins, GRA2 and SAG1 to heparin, additional heparin-agarose affinity column binding assays were performed using a total cell lysate preincubated with heparin. Under these conditions, GRA2 and ROP

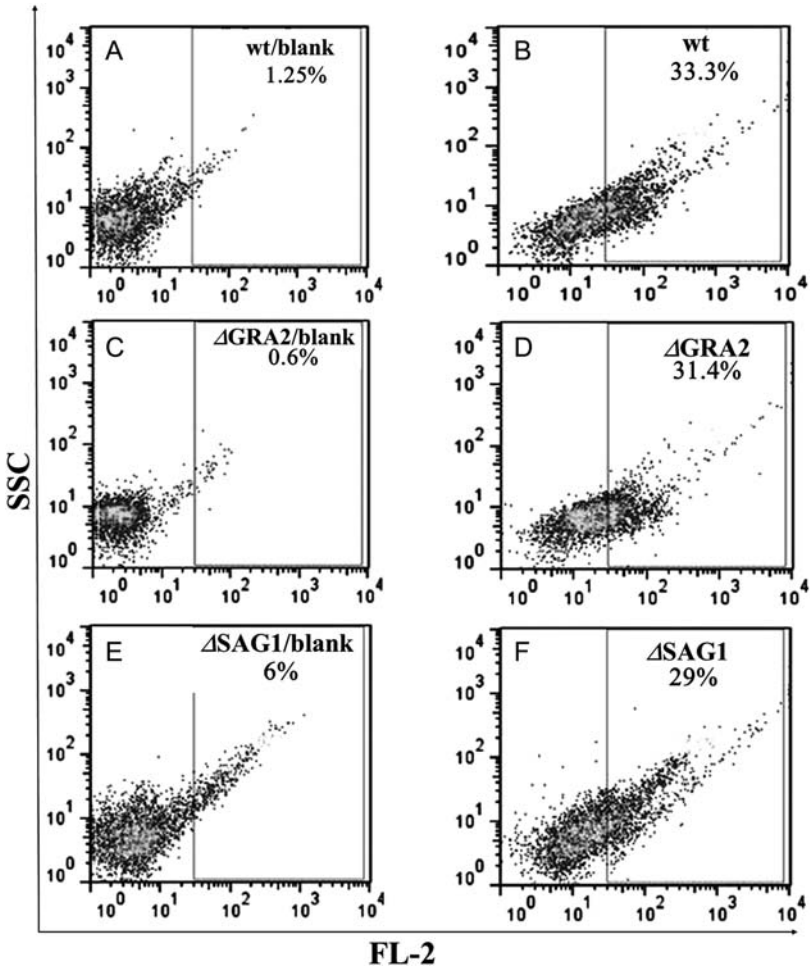

Fig. 3. Quantification of the binding of heparin to *T. gondii* tachyzoites. The percentage of positive cells is indicated in the top right hand corner of each graph. Purified wt RH tachyzoites and mutants of the *T. gondii* deficient for the surface protein SAG1 and GRA2 (ΔSAG1 and ΔGRA2) were incubated for 10 min with 10 μM zeolite functionalized with or without (blank) heparin, the binding was measured by flow cytometry. Excitation wavelength in the FACS experiments was 540 nm, which is the excitation wavelength of rhodamine B. Cells were gated on living cells and fluorescence channel FL-2 (PE-A) was used to detect tachyzoites that had binded rhodamine B-labeled heparin-functionalized zeolite.

proteins were not retained by the column (Figure 4B), demonstrating that treatment with soluble heparin abolished binding between immobilized heparin and the lectins. This further confirmed the affinity of these proteins to heparan sulfate structures.

Microarray screen of synthetic, sulfated heparin oligosaccharides

A synthetic oligosaccharide microarray was used to investigate the minimal oligosaccharide structure, as well as the optimal sulfation pattern, that could support binding of *T. gondii* rhoptry and dense granule proteins. A series of di-, tetra- and hexasaccharides of the glucosamine-iduronic acid (GlcN-IdoA) repeating unit of the major sequence of heparin were synthesized. Different sulfation patterns were introduced via position 2 of the iduronic acid units and positions 2 and 6 of the glucosamine units. The library contained 13 structures with different charge and spatial orientation patterns (Figure 5). Functionalized deaminated heparin obtained from natural sources with an average molecular weight of 5 kDa was also included (Figure 5, structure **14**). Each microarray slide was incubated with a concentration of 10–20 μg of either immunopurified ROP proteins or purified recGRA2 protein. The observed shift of the molecular weight of recGRA2 (34 kDa) compared with a molecular weight of native GRA2 (28.5 kDa; Mercier et al. 1993) is due to the His-tag having a molecular weight of around 6 kDa. There were overall similarities in the fluorescence patterns obtained from incubation with either the ROP proteins or recGRA2, indicating that these proteins bind some common synthetic heparin oligosaccharides (Figure 6). However, there were some noticeable differences in the specificities of the various lectin-oligosaccharide interactions and in the intensities of the resulting fluorescence signals, suggesting that the ROP proteins and recGRA2 have affinities for different structural epitopes. The distinct features of the binding patterns allowed us to rule out the possibility that the binding was a result of non-specific interactions. Furthermore, non-specific interactions were unlikely because the fluorescence signal intensities decreased as

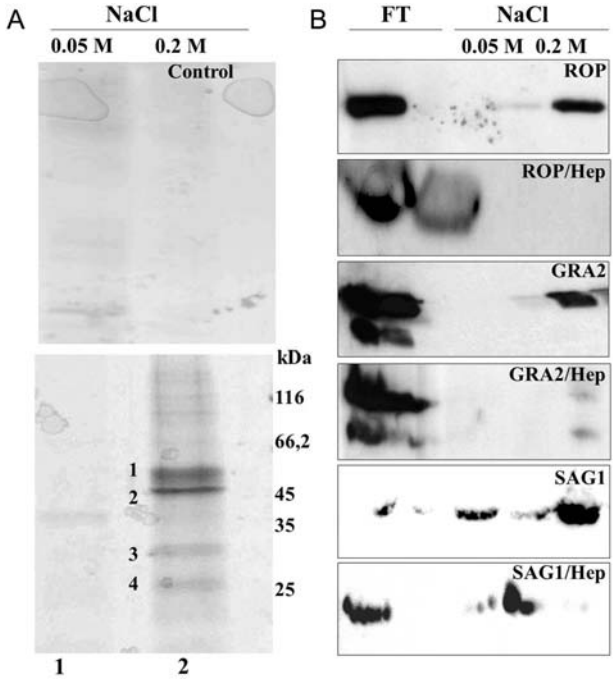

Fig. 4. Identification of *T. gondii* heparin-binding proteins. (**A**) Coomassie-stained SDS–PAGE profile of *T. gondii* proteins isolated after heparin-agarose affinity chromatography (bottom panel) or as a control, after non-functionalized agarose chromatography (top panel). Protein bands 1–4 eluted with 0.2 M NaCl (lane 2) were subjected to peptide mass fingerprinting. kDa corresponds to molecular weight markers. (**B**) Immunoblot profiles of proteins eluted from a heparin agarose column in the absence of or after 2 h preincubation with heparin at a final concentration of 1 mg/mL. Western blot analyses were performed with the mAbs anti-GRA2, anti-ROP proteins or anti-SAG1. FT, flow-through; Hep, heparin.

the spotted sugar concentrations decreased. Overall, the microarray fluorescence patterns showed that ROP proteins bound more glycan structures than recGRA2. ROP proteins bound lower concentrations of oligosaccharide than recGRA2, supporting the hypothesis that ROP proteins bind heparin more tightly than recGRA2. Both the ROP proteins and recGRA2 commonly recognized and tightly bound the longer oligosaccharides (**1**, **2**, **5** and **7**), as well as 2,4-sulfated iduronic acid (**11**), which bears an unnatural sulfation pattern, and natural heparin (**14**) (Figure 6). These synthetic structures are all highly sulfated, bearing at least two sulfates per disaccharide unit, and most closely resemble natural heparin. Oligosaccharide **2**, however, displays a modification pattern that cannot be found in mammals because glucuronosyl C5 epimerases do not act on glucuronic acids adjacent to *N*-acetylated glucosamine moieties (Bäckström et al. 1979). Less sulfated and non-sulfated structures (**3**, **4**, **6**, **8**, **9** and **13**) showed either weak or no binding. Therefore, strong ionic interactions between the *T. gondii* proteins and the synthetic oligosaccharides are important for recognition and binding by ROP proteins and recGRA2. Interestingly, recGRA2 did not bind the highly sulfated monosaccharides **10** and **12**, which were bound by the ROP proteins. The affinity of the ROP proteins to the highly charged oligosaccharides **10** and **12** implies that electrostatic interactions are even more important for ROP proteins than for recGRA2. In summary, together, the data clearly point out the influence of the number of sulfate groups and their specific distribution within the heparin chain for binding the ROP and recGRA2 proteins. As an additional control, competition binding assays were performed, where recGRA2 and the ROP proteins were incubated with 5 mM deaminated heparin prior to the microarray experiments. Figure 6 clearly shows that preincubation with heparin abolished the binding of both proteins to the printed glycan structures.

As shown above in inhibition assays using sag1 KO mutant, the parasite surface protein SAG1 is one candidate for the first protein that interacts with the host cell GAG structures. Furthermore, the crystal structure of the SAG1 protein revealed a positively charged groove which seems to be conserved among *T. gondii* cell surface GPI-protein family that may bind to sulfate molecules of GAG structures (He et al. 2002). Therefore, binding specificities of immunopurified SAG1 were also evaluated using the synthetic heparin microarray used previously. Figure 6 shows the fluorescence patterns resulting from immunopurified SAG1 binding to the glycans. SAG1 tightly bound to the longest structures (**1**, **5**, **6** and **7**), as well as to natural heparin **14**. SAG1 binds also more tightly to shorter structure (**10**, **11** and **12)** oligosaccharides. All the structures bound by SAG1 are highly sulfated which supports our hypothesis that charged sulfate groups play an important role in these protein–glycan interactions. The primary difference between binding specificities of the ROP and GRA2 proteins and that of SAG1 is that the density of sulfate groups seems to be more important for the SAG1 binding rather than the overall number.

Binding specificities of recROP2 and recROP4

As the secretory organelles of *T. gondii* are known to be actively involved in the invasion process, we were particularly interested in elucidating the function of the secretory proteins during the early steps of the invasion, and therefore, we focused our attention once again on the ROP proteins. Two recombinant (Rec) ROP proteins were expressed and purified, recROP2 and recROP4, which lack the first 194 and 155 amino acids of their native protein sequences, respectively. The carbohydrate-binding specificities of recROP2 and recROP4 were assessed using the synthetic heparin microarray to determine whether these Rec proteins have the same binding pattern as the affinity purified natural ROP proteins. Since both Rec proteins were N-truncated, comparison with the heparin-binding pattern of natural ROP proteins may reveal whether crucial heparin-binding sites are located within the N- or C-terminal domains. Figure 7 shows that recROP2 and recROP4 bound the synthetic heparin microarray similarly, and in fact, their binding patterns were comparable with that observed with the natural ROP proteins (compare Figure 7A and B with Figure 5). Together, the data using native proteins and the N-truncated Rec proteins, we concluded that the heparin-binding sites are located in the C-terminal domains of the ROP proteins. However, additional truncated constructs of these proteins such as C-truncated proteins are needed to support this hypothesis.

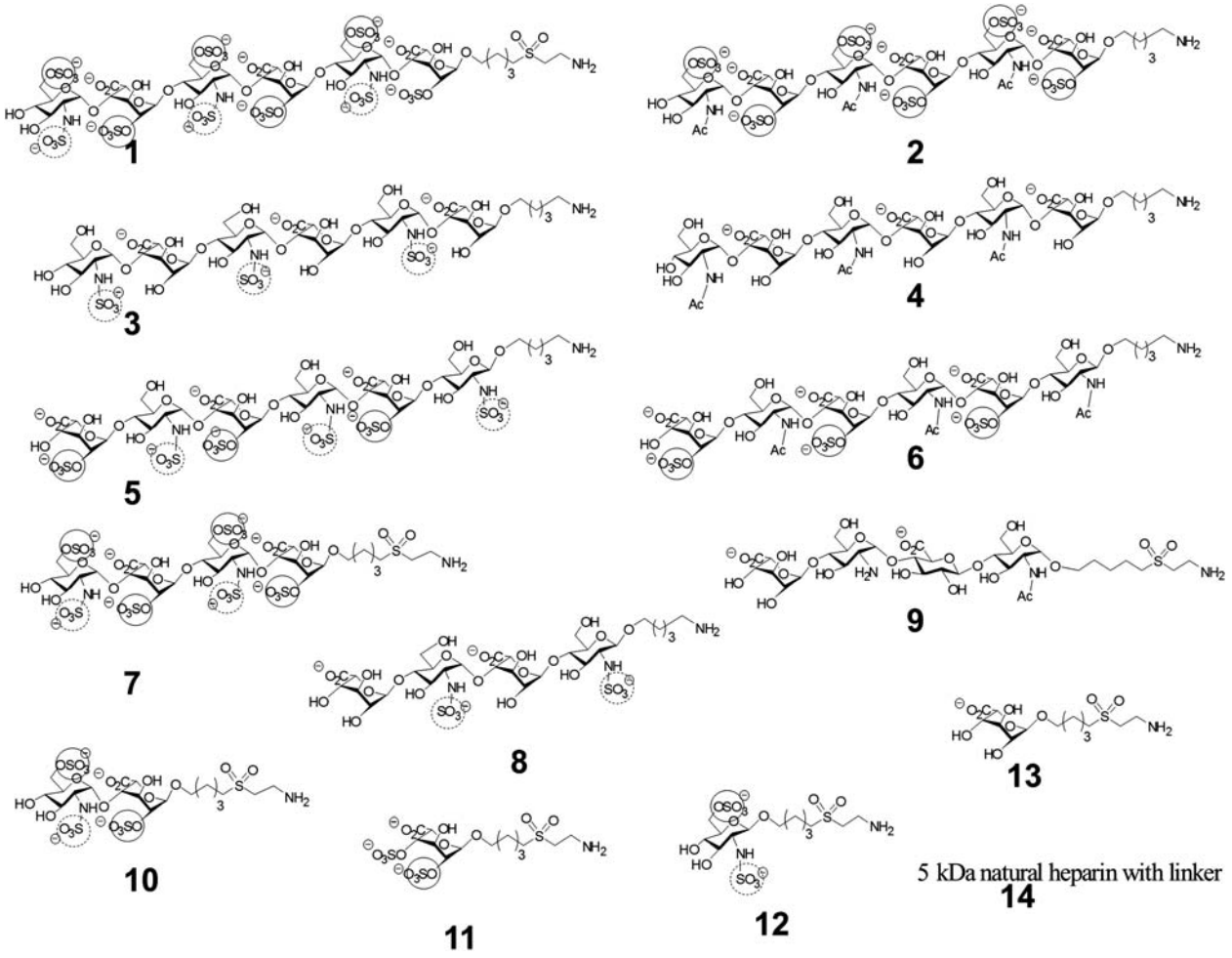

Fig. 5. Sulfated heparin oligosaccharides and heparin from natural sources. A series of di-, tetra- and hexasaccharides containing the GlcN-IdoA disaccharide (structure **10**) repeating motif of the major sequence of heparin. The structures are equipped with an amine-terminated linker at the anomeric position of the reducing end for immobilization purposes. Different sulfation patterns involve position 2 of the iduronic acid units and positions 2 and 6 of the glucosamine units.

Next, the kinetics of ROP–heparin binding was investigated by measuring the interactions between either recROP2 or recROP4 and immobilized natural heparin using SPR. Each experiment comprised of six injections of different concentrations of either recROP2 or recROP4 (Figure 7C and D). Additionally, either 5 μM recROP2 or 0.45 μM recROP4 proteins preincubated with increasing concentrations of natural 5 kDa heparin was injected as a control (Figure 7E and F). The sensorgrams revealed a binding interaction between recROP proteins and immobilized natural heparin, and as expected, this interaction was increasingly inhibited by preincubation with increasing concentrations of heparin. The K_D calculated from the experimental kinetic data (Table I) of recROP2 and recROP4 for natural heparin were 0.43 and 0.016 μM, respectively. These K_D values, while low, are within in the range expected for lectin–carbohydrate interactions (Lee and Lee 1995). Relatively weak binding reflects invasion events that are often rapid, transitory and involve limited numbers of cells.

To validate the assumption that our synthetic heparin structures could be useful in future experiments, such as in vivo inhibition assays, the binding of recROP2 and recROP4 to immobilized hexasaccharide **1** was also measured by SPR. In this case, each SPR binding experiment was comprised of three injections of either recROP2 or recROP4 at different protein concentrations. The sensorgrams revealed binding interactions between each recROP protein and synthetic hexasaccharide **1** (Figure 7G and H). However, further characterization of the interaction between the synthetic oligosaccharides and ROP proteins such as the determination of binding kinetics are needed. Also, additional binding inhibition assays using different synthetic heparin oligosaccharides instead of natural heparin will be useful for identifying highly potent inhibitors.

Discussion

Prior to this investigation, it was known that *T. gondii* secretory proteins were essential for invasion and that heparin-like molecules were inhibitors of this process. However, a link between these independent observations has not yet been

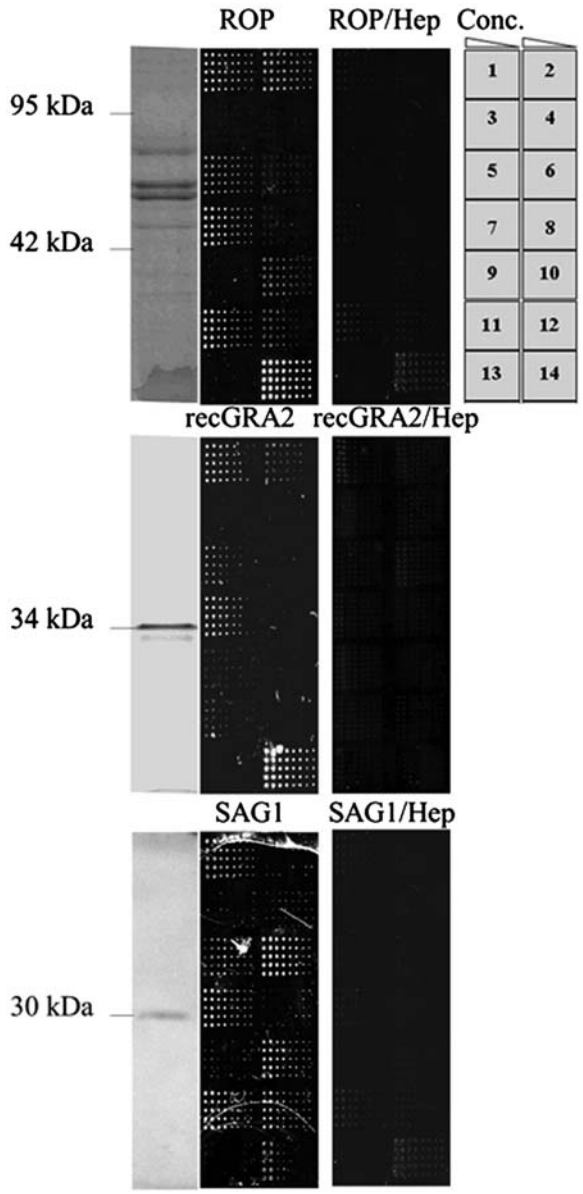

Fig. 6. Heparin oligosaccharide microarray analyses of immunopurified ROP proteins, SAG1 and of recGRA2. Fluorescence images obtained from the array scanner after incubating the heparin oligosaccharide microarray with *T. gondii* immunopurified ROP proteins, SAG1 or recGRA2, and the corresponding inhibition controls performed by preincubating the purified proteins with 5 mM soluble heparin. Each sugar was printed in duplicate spots, in five replicas on the slide, at four different concentrations ranging from 1000, 250, 63 to 16 μM. The left lanes correspond to Coomassie-stained SDS–PAGE of the immunopurified proteins. Hep, heparin; Conc., concentration.

reported. Here, we provide evidence that proteins from the tachyzoite secretory organelles, rhoptries and dense granules are heparin-binding lectins. Interestingly, microneme proteins, which are considered to be a major class of *T. gondii* cellular adhesins (Barragan et al. 2005; Carruthers and Tomley 2008; El Hajj et al. 2008; Soldati-Favre 2008), were not identified by heparin affinity chromatography, confirming that these proteins have an affinity for sialic acid-containing cell surface molecules. Indeed, the heparin- and sialic acid-based invasion pathways were thought to be simultaneously accessible and independent. Accordingly, in this report, we observe that even relatively high concentrations of free heparin were not able to completely inhibit parasite invasion, most likely because the sialic acid-dependent invasion pathway was not disrupted (Figure 1). It is therefore evident that the interaction between the parasite and the host cell is multifaceted and concomitantly mediated by multiple adherence factors.

The role of the binding of rhoptry and dense granule proteins to host cell GAGs during infection process is not fully understood, particularly in the case of GRA proteins. GRA2 secretion occurs at the end of the invasion process, suggesting its involvement in intracellular parasite development and multiplication in the parasitophorous vacuole (Cesbron-Delauw et al. 2008). The membrane form of GRA2 linked to a nanotubular network is mediated by two amphipathic α-helical domains (Mercier et al. 1998). The initial binding to a negatively charged component of the membrane is mediated by the net positive charge of each GRA2 amphipathic α-helix. Although the binding of GRA proteins to the heparan sulfate structure has never been investigated, it was reported that heparan sulfate facilitates the replication of *T. gondii* in the parasitophorous vacuole (Bishop et al. 2005). However, it is logical that the most important binding event occurs during the initial contact between the tachyzoite and the host cell and is, in part, mediated by the tachyzoite SAG family of surface protein and host cell proteoglycans. Binding between heparan sulfate and surface antigens, such as SAG1, may help to establish initial contact between the parasite and the host. We have shown that the *T. gondii* surface protein SAG1 binds heparin as does SAG3 (Jacquet et al. 2001). In addition, by imaging a direct interaction between tachyzoites and heparin-coated zeolites using confocal force microscopy and AFM, this report supports the hypothesis that the initial contact is mediated by a heparan sulfate-binding event (Figure 6). An earlier observation showing that anti-SAG1 antibodies inhibited infection by *T. gondii* further substantiates this hypothesis (Velge-Roussel et al. 2001). Interaction between protein components of the rhoptries (ROP2, ROP4 and ROP5) or dense granules (such as GRA2) and GAGs, as reported here, most likely occur after the initial contact is established and may coordinate efficient entry of parasites into host cells. Rhoptries and other secretory organelles have been shown to play an important role in the early steps of host cell invasion by Apicomplexa parasites (Saffer et al. 1992; Dubremetz et al. 1998; Carruthers et al. 1999; Menard 2001).

We demonstrated that rhoptry and dense granule proteins bind to sulfated heparin oligosaccharides with unique specificities that probably reflect the fact that these proteins do not share a high sequence homology. The affinity of a protein for each synthetic oligosaccharide is determined by a combination of the overall oligosaccharide conformation as well as charge distribution and flexibility. In particular, we observed that the location of the sulfated residues was as important as the global charge density: 2-O-sulfation of iduronic acid was necessary but not sufficient for rhoptry and granule protein binding. However, N-sulfation or 6-O-sulfation on

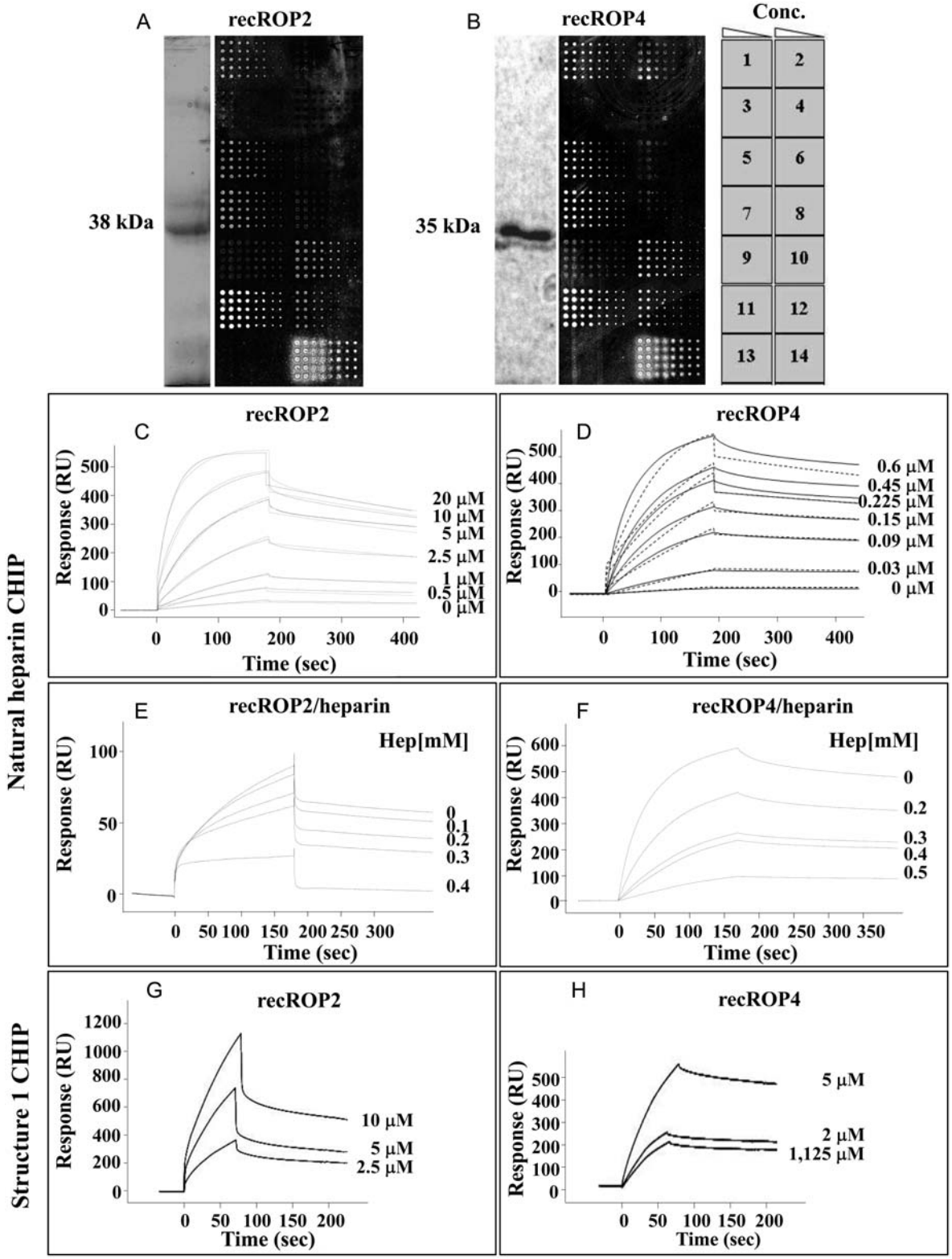

Fig. 7. Binding analyses of recROP2 and recROP4. (**A** and **B**) Coomassie-stained SDS–PAGE analyses of affinity purified recROP2 and recROP4 proteins and their corresponding heparin oligosaccharide microarray analyses. (**C** and **D**) SPR sensorgrams for recROP2 and recROP4 interactions with immobilized natural heparin. The purified protein samples contained increasing concentrations of recROP2 and recROP4, as indicated. These data were used to determine the kinetics of the interaction. The solid lines indicate the experimental curves and the dashed lines the fitting curves. (**E** and **F**) SPR sensorgrams of the same interaction after preincubation of the recROP2 and recROP4 with increasing concentrations of soluble heparin from natural sources. The concentrations of recROP2 and recROP4 were 4 and 0.45 µM, respectively. The concentrations of heparin were as indicated. (**G** and **H**) SPR sensorgrams for recROP and recROP4 interaction with synthetic heparin oligosaccharide **1**.

Table I. SPR kinetic data for recROP proteins

Proteins	k_a (M^{-1} s^{-1})	k_d (s^{-1})	K_D (M)	R_{max} (RU)
recROP2	2.027×10^3	8.813×10^{-4}	4.349×10^{-7}	429.3
recROP4	4.431×10^4	7.016×10^{-4}	1.583×10^{-8}	513.6

k_a, association rate constant in M^{-1} s^{-1}; k_d, dissociation rate constant in s^{-1}; K_D, equilibrium dissociation constant in M; R_{max}, maximal response in RU; RU, response units.

glucosamine was essential, with N-sulfation seeming to be more important than *O*-sulfation. Overall, two or more sulfate groups per disaccharide unit throughout the structure were crucial for tight binding. Moreover, the sulfate groups need to be present on the same monosaccharide residue of each disaccharide unit for optimal activity.

Despite the relatively small collection of synthetic heparin oligosaccharides in our library, it is now possible, as demonstrated here, to prepare structurally defined oligosaccharides and we have demonstrated the power of this tool for investigating heparin function at the molecular level. The analysis of structurally defined oligosaccharides allows for a comparison of different modification patterns and for the determination of absolute affinities between the binding proteins and defined oligosaccharide structures.

Protein glycosylation does not impact the interaction of parasite proteins with synthetic heparin oligosaccharides, since microarray and/or SPR binding experiments were conducted using non-glycosylated Rec proteins. The N-glycosylation pathway in Apicomplexa such as *T. gondii* is underrepresented or non-existent (Garénaux et al. 2008).

A lack of effective anti-parasite vaccines means that parasitic infections are still the cause of major global health problems. The situation is further complicated because parasites are developing resistance to currently available drugs, and the side effects of these treatments are debilitating. New therapies are needed, and a comprehensive understanding of the molecular basis of the host–pathogen interaction will be crucial for the rational design of targeted anti-parasitic drugs. Our report represents a first step in demonstrating the potential for targeting host cell invasion by *T. gondii* in the development of therapeutic approaches as well as anti-parasitic drugs and vaccines. Structural and molecular characterization of the heparin-binding sites will provide new insights into the interface between the parasite and the host and enable the selection of effective antigenic epitopes for vaccine development that will generate antibodies with potent anti-parasitic inhibitory activity. Alternatively, specific heparin-based drugs may come within reach as a result of a better understanding of the structure–function relationships.

Materials and methods

Parasites and cell culture

Toxoplasma gondii: RH and mutant of the *T. gondii* RH tachyzoites deficient for the surface protein SAG1 (provided by Dr Michael Grigg and Dr John Boothroyd, Stanford University) and RH tachyzoites deficient for GRA2 (Travier et al. 2008) strains were grown in Vero cells (ATCC CCL-81). Vero cells were cultured in Dulbecco's modified Eagle's medium (DMEM; Gibco BRL, Germany), supplemented with 10% fetal calf serum (FCS; Gibco), 2 mM glutamine, 100 U/mL penicillin and 0.1 mg/mL streptomycin. Confluent cell cultures (T175 cm^2) were infected with 5×10^7 tachyzoites in DMEM supplemented with 1% (v/v) FCS. Tachyzoites were harvested after 72 h. They were released by bursting their host cells using the Mixer Mill homogenizer with glass beads (Retsch, Germany). The suspension was filtered through a 2-mL glass wool column to remove cellular debris. The purity of the parasite suspension was monitored by confocal microscopy.

Synthesis of N,N′*-bis(2,6-dimethylphenyl) perylene 3,4,9,10-tetracarboxylic diimide, aminated zeolites and bifunctional zeolites*

Zeolites equipped with the green fluorescent emitter *N*,*N*′-bis (2,6-dimethylphenyl) perylene 3,4,9,10-tetracarboxylic diimide and amino groups were synthesized following previously published procedures (Strassert et al. 2008; Guerrero-Martinez et al. 2009). Deaminated heparin (5 mg) was added to 1 mL of amino-zeolite in water. The mixture was stirred at room temperature for 12 h. Rhodamine B isothiocyanate (5 mg, 9.3 μM) was added to the reaction mixture after 3 h. To remove the uncoupled heparin and rhodamine B, the solution was submitted to cycles of ultrafiltration at 10,000 × *g* on Microcon with a cutoff of 10 kDa. The solution was washed three times with 100 mM bicarbonate buffer, concentrated to a final volume of 500 μL and stored at −20°C until use. The control zeolite polymers were made by omitting the heparin addition step.

Estimation of the concentration of heparin and rhodamine on zeolite

The concentration of heparin sugar on the polymer was determined by the carbazole assay (Bitter and Muir 1962) using a microtiter plate. 0.1 mg/100 μL of heparin-functionalized zeolite solution was mixed with 25 μL of concentrated sulfuric acid and 50 μL of an aqueous carbozole reagent. The mixture was added to the microtiter plate and heated to 80°C. After 15 min, the plate was cooled to room temperature and the absorbance was measured at 530 nm using an Infinite M200 NanoQuant microplate reader (Tecan, Switzerland). A standard curve was built using serial dilutions of heparin. The heparin concentration was estimated by comparing the absorption of the sample with the standard curve. Compound **1** showed 0.32×10^{-6} M of heparin per 1 mg of zeolite. The rhodamine B concentration was determined using the rhodamine B molar extinction coefficient of 106,000 M^{-1} cm^{-1} at 542 nm and the optical density of the compound **1**. Compound **1** showed 0.75×10^{-5} M rhodamine B concentration per 1 mg of zeolite.

Preparation of mica surface and samples for AFM measurements

Mica surfaces were prepared according to the procedure reported by Doktycz et al. (2003). A gelatin solution was prepared by dissolving 0.5 g of gelatin (Sigma-Aldrich, Germany) and 10 mg of chromium ammonium sulfate in 100 mL of water at 60°C. After cooling to 40°C, a mica disk was vertically dipped into the solution and dried overnight. After incubation

with heparin-functionalized zeolite, the suspension of parasites was centrifuged to pellet the cells and washed four times with a PBS buffer (4 × 400 mL of buffer) to remove the excess of zeolite. An aliquot of 20 mL of zeolite-labeled parasites was loaded onto the gelatin-treated mica disk. After 30 min, the disk was rinsed with water (2 × 50 mL) and allowed to dry for air imaging. AFM was performed with a multimode instrument with a Nanoscope IIIa controller (Veeco Instruments, Germany) operating in the tapping mode. The samples were placed onto the Mica disk and tipped (Nano world tip) with a spring constant of 42 N/m and a resonance frequency of 285 kHz.

Confocal microscopy

Toxoplasma gondii RH-88 strain RF-GFP 5 S65T (ATCC-50940) that stably expresses the GRA1-GFP protein was grown in Vero cells and purified as described in parasites and cell culture paragraph. Purified tachyzoites were washed with the PBS buffer and fixed for 10 min with 4% (w/v) paraformaldehyde. After incubation for 30 min with zeolite functionalized either with or without heparin, the suspension of parasites was centrifuged to pellet the cells, washed four times with PBS buffer (4 × 400 mL) to remove the excess of zeolite, and finally, cells were suspended in PBS buffer. An aliquot of 20 mL of the parasite-zeolite suspension was spotted onto a slide and mounted in Fluoroprep (Dako, Germany). Imaging analyses were performed using an LSM 700 confocal scanning microscope (Zeiss, Germany).

Metabolic labeling of tachyzoites

Confluent Vero cell cultures were infected for 72 h, washed twice with glucose-free DMEM containing 20 mM sodium pyruvate. Parasite glycans were labeled using the same media supplemented with 0.5 mCi D-[6-^{3}H]glucosamine (Amersham Biosciences, Germany) for 6 h at 37°C. [^{3}H]glucosamine labeling was chosen for its rapid incorporation into cell surface glycoproteins and glycolipids. After labeling, parasites were liberated from host cells and purified as described in parasites and cell culture paragraph.

Toxoplasma gondii infection assays

Vero cells were harvested in DMEM, plated in duplicate at a density of ~1×10^5 cells/well in 24-well plates and incubated for 12 h at 37°C in the presence or the absence of $NaClO_3$, a reversible inhibitor of adenosine 3′-phosphoadenylylphosphosulfate and proteoglycan sulfation (Humphries and Silbert 1988), to a final concentration of 20 or 50 mM. In competition assays, purified tachyzoites were incubated with heparin, bovine trachea CS-A, porcine intestinal mucosa CS-B (dermatan sulfate) from Sigma-Aldrich, hypoS fucoidans derivative of native brown alga *F. evanescens* fucoidan prepared by solvolytic desulfation of native fucoidan by treatment of its pyridinium salts with dimethyl sulfoxide containing 10% of methanol at 100°C for 3 h (Khil'chenko et al. 2011) or trimannose oligosaccharide for 10 min at 37°C prior to infection. Monolayers were washed with cold DMEM and analyzed as below. For *T. gondii* attachment/invasion assays, purified [^{3}H]glucosamine-labeled tachyzoites were harvested, suspended in PBS buffer, pH 7.2, and 0.2 mL of the parasite suspension was added to Vero cell monolayers in duplicates and incubated at 37°C. After a period of incubation of 1 h, cells were harvested and washed extensively in PBS buffer, pH 7.2, to remove non-attached parasites. *Toxoplasma gondii* infection levels were determined by suspending the infected monolayer in Tris–HCl buffer containing 1% Triton X-100 followed by measuring the emitted radiation after amplifying the signal with scintillation liquid.

Flow cytometry quantification of heparin-functionalized zeolite binding

Purified wt RH tachyzoites and mutants of the *T. gondii* RH tachyzoites deficient for the surface protein SAG1 and GRA2 were plated in 6-well plates and cultivated in DMEM, supplemented with 10% FCS, 2 mM glutamine, 100 U/mL penicillin and 0.1 mg/mL streptomycin. Tachyzoites (5×10^6) were washed with PBS buffer and fixed for 30 min with 4% (w/v) paraformaldehyde at room temperature (RT) and washed with PBS buffer. After incubation for 10 min with zeolite functionalized either with or without heparin, the suspension of parasites was centrifuged to pellet the cells, washed five times with PBS buffer. The binding was measured by flow cytometry using a FACSCantoTM II flow cytometer (Becton Dickinson, Germany). The excitation wavelength in the fluorescence activated cell sorting (FACS) experiments was 540 nm, which is the excitation wavelength of rhodamine B. Cells were gated on living cells and fluorescence channel FL-2 (PE-A) was used to detect tachyzoites that had binded rhodamine B-labeled heparin-functionalized zeolite. All data were analyzed with the FlowJo software (Tree Star. Inc., Ashland, OR).

Identification of T. gondii heparin-binding proteins

Purified tachyzoites (1×10^9) were lysed in 50 mM Tris–HCl containing 0.01 mM leupeptin, 0.25 mM phenylmethylsulfonylfluorid (PMSF), 1 mM ethylenediaminetetraacetic acid (EDTA), pH 7.4, containing 1% Triton X-100. After 1 h at 4°C, the supernatant was separated from the pellet by centrifugation at 20,000 × *g* for 15 min at 4°C. The supernatant was dialyzed overnight against 50 mM Tris–HCl, 5 mM EDTA, pH 7.4. A volume equivalent to 1×10^8 parasites was applied into a 1-mL syringe packed with heparin of a molecular weight between 25 and 35 kDa linked to agarose. The column is equilibrated in buffer A: 50 mM Tris–HCl, 5 mM EDTA, 10 mM NaCl, pH 7.4, containing 0.2% Triton X-100. The column was then incubated for 1 h at 4°C. Unbound proteins were removed by washing the column with 5-column volumes of equilibration buffer A. Weakly bound proteins were eluted with 5-column volumes of equilibration buffer A containing 0.05 M NaCl. Elution of strongly bound proteins was carried out using 3-column volumes of equilibration buffer A containing 0.2 M NaCl. The column was regenerated by washing with 5-column volumes of equilibration buffer A containing 2 M NaCl, followed by 4 column volumes of equilibration buffer A. An aliquot of 200 µL from each eluted fraction was submitted to acetone precipitation. Protein pellets were suspended in Laemmli buffer and resolved using 12.5% SDS–PAGE (Laemmli 1970) under non-reducing conditions. After Coomassie staining, the major protein bands were excised, destained and reduced prior to tryptic digestion and peptide mass fingerprinting. Matrix-assisted laser desorption/ionization (MALDI) mass spectra were generated using a

Voyager DE-STR matrix-assisted laser desorption/ionization-time of flight- mass spectrometry (MALDI-TOF MS) system (Applied Biosystems, USA) with delayed extraction in the reflectron mode. Proteins were identified by comparison of peak lists generated from the Data Explorer application (PerSeptive Biosystems) against NCBInr and Swiss-prot databases using the Protein-Prospector V3.4.1 software MS-Fit (http://www.prospector.ucsf.edu).

Expression and purification of RecGRA2, RecROP2 and RecROP4 proteins and immunopurification of ROP proteins and SAG1

Escherichia coli BL21 cells transformed with the construct *pUET*-GRA2 were grown at 33°C until they reached an OD_{600} of 0.4–0.5 according to the methods described by Golkar et al. (2007). Expression was induced for 4 h at 37°C by addition of isopropyl β-D-thiogalactoside to a final concentration of 1 mM. Bacteria were harvested by centrifugation at 6000 × *g* for 20 min at 4°C. The bacterial pellet was solubilized in 8 mL of lysis buffer [0.5 mM imidazole, 5 mM NaCl, 20 mM Tris–HCl, pH 8.3, 0.1% Triton X-100, 2 tablets/L of protease inhibitor cocktail (Sigma-Aldrich) without EDTA, 1 mg/mL lysozyme]. The cells were broken by sonication for 6 min using an (MSE, London, UK) ultrasonic disintegrator at 60% of power and centrifuged. The supernatant was applied onto a Ni^{2+}-NTA column (Qiagen, Germany) equilibrated with a buffer containing 500 mM NaCl, 20 mM Tris–HCl, pH 8.3, 0.01% Triton X-100. Recombinant GRA2 (RecGRA2) was eluted from the column by successively applying 1 mL of the following solutions: W20 (20 mM imidazole, 500 mM NaCl, 20 mM Tris–HCl, pH 8.3, 0.01% Triton X-100); W40 (same as W20 but with 40 mM imidazole); W60 (same as W20 but with 60 mM imidazole). *Escherichia coli* BL21 transformed with the Rec plasmid pHis-ROP2 or pHis-ROP4 were grown in lysogeny broth (LB) supplemented with 100 µg/mL ampicillin to an OD_{600} of 0.6, followed by the induction with 0.5 mM isopropyl β-D-thiogalactoside for 3 h at 37°C. Recombinant proteins were purified as reported (Dziadek et al. 2009). Immunoaffinity purification of ROP and SAG1 proteins was accomplished following methods described by Zinecker et al. (2001). Briefly, 2×10^{10} tachyzoites were purified using glass wool columns and lysed for 1 h in 50 mM Tris–HCl pH 8.3, containing 150 mM NaCl, 0.5% NP40, 2 mM EDTA and protease inhibitor cocktail (Sigma-Aldrich). The lysate was cleared by centrifugation and circulated for 24 h over 1 mL of CNBr-sepharose coupled to mAbs specific for ROP2/4/5 or SAG1. After washing, the bound material was eluted with 0.01% Na-deoxycholate in 0.1 M diethylamine–HCl, pH 11.5. Purified proteins were dialyzed against PBS buffer, pH 7.2. The Rec proteins were refolded by a one step 10-fold dilution in PBS buffer (pH 7.2). Protein concentrations were determined using a bicinchoninic acid (BCA) protein assay kit reagent (Thermo Scientific; Germany) and purity was assessed by 12.5% SDS–PAGE.

Immunoblotting and antibodies

Immunoblots were performed by successive incubations with primary mouse mAbs and then with secondary horseradish peroxidase (HRP)-conjugated anti-mouse IgG. Immunoreactivity was determined after incubation with the enhanced chemiluminescence detection reagents. The following mAbs were used for western blotting, immunoaffinity purification of native proteins and microarray experiments: TG 17.179 anti-GRA2 (Charif et al. 1990; Cesbron-Delauw et al. 1992), T3 4A7 anti-ROP2 and anti-ROP4 (Sadak et al. 1988; Leriche and Dubremetz 1991) and T4 1E5 anti-SAG-1 (Couvreur et al. 1988).

Preparation of sulfated heparin oligosaccharides

Deaminated 5 kDa heparin (Santa Cruz Biotechnology, Santa Cruz, CA) was prepared by nitrous acid deamination of porcine intestinal mucosal heparin according to Kosakai et al. (1978). Heparin oligosaccharides **1**–**13** were prepared and characterized as described previously (de Paz et al. 2006; Noti et al. 2006). Heparin oligosaccharide **9** was synthesized and characterized according to the published procedures (Adibekian et al. 2007). Heparin oligosaccharide **14** was prepared by functionalization of deaminated 5 kDa heparin with 1,11-diamino-3,6,9-trioxaundecane by reductive amination. Heparin oligosaccharides were dissolved in 50 mM PBS buffer, pH 8.5, and robotically printed using a piezoelectric spotting device (S11, Scienion, Berlin, Germany) onto *N*-hydroxysuccinimide (NHS)-activated CodeLink slides (Amersham Biosciences), in 75% relative humidity, at 23°C. One nanolitre of each oligosaccharide was printed at four different concentrations ranging from 1000, 250, 63 to 16 µM, in duplicate and in five replicas on the slide onto the activated slides using a robotic printer to give average spot sizes of 200 µm. Immobilization of the structures on CodeLink-activated ester slides yielded a signal-to-noise ratio of ≥10. Slides were stored in an anhydrous environment. Prior to the experiment, the slides were washed three times with water and the remaining succinimidyl groups were quenched by incubating the slides in 100 mM ethanolamine in 50 mM PBS buffer (pH 9) for 1 h at 50°C. The slides were then rinsed three times with water and dried by centrifugation.

Microarray binding assays

Glycan microarray incubations were performed as follows: 100 µL containing 10–20 µg of either recGRA2, recROP2, recROP4, affinity-purified native ROP proteins or affinity-purified SAG1 in PBS buffer containing 0.05% Tween-20 and 0.5% bovine serum albumin (BSA), were placed between array slides and plain coverslips and incubated for 2 h at RT. Control incubations were performed under the same conditions except the proteins were preincubated with heparin at a final concentration of 1 mg/mL. The arrays were washed with buffer A (10 mM PBS buffer, pH 7.5, containing 1% Tween-20 and 0.1% BSA), twice with water and then centrifuged for 5 min to remove excess buffer. Slides were then incubated with the corresponding mouse mAb for 1 h at RT. After intensive washing with buffer A, the slides were incubated for 1 h at RT with ALEXA-Fluor® 594-labelled anti-mouse antibody (Invitrogen, Germany) at 1:1000 in 10 mM PBS buffer containing 0.5% BSA and 0.05% Tween-20, followed by washing with buffer A. An Affymetrix 427 laser scanner (MWG Biotech, Santa Clara, CA) was used to detect immunofluorescence.

Kinetic analysis by SPR assays

Experiments were conducted using a Biacore T100 (GE Healthcare, Uppsala, Sweden). Heparin oligosaccharide **1** and 5 kDa natural heparin were immobilized on the carboxymethylated dextran CM5 chips. For the immobilization of the natural heparin or heparin oligosaccharide, the dextran matrix was activated with a mixture containing 200 mM *N*-ethyl-*N*′-(dimethylaminopropyl)carbodiimide and 50 mM NHS for 7 min directly followed by the amine-functionalized oligosaccharide. Exposed amines in the solution could then react with succinimide esters to form a covalent linkage. The concentration was adjusted to 50 μg/mL in water supplemented with 1 mM hexadecyltrimethylammonium chloride. The contact times were 7–9 min which resulted in responses between 1200 and 1300 response units. Immediately after the last injection, free NHS groups were quenched by a 7-min injection of 1 M ethanolamine. Importantly, as reference, at least one flow cell of a chip was activated and subsequently quenched to correct effects of a signal drift, non-specific binding and other bulk effects during injections. Unless otherwise noted, flow rates of 10 μL/min were used for analyses as well as coupling, 30 μL/min for regeneration, and the running buffer was hepes buffer saline buffer (10 mM (4-(2-hydroxyethyl)-1-piperazineethanesulfonic acid) (HEPES), pH 7.4, 150 mM NaCl). To determine the K_D between immobilized heparin oligosaccharides and recROP2 or recROP4, respectively, proteins at different concentrations were injected over the sensor surface. The association time was 3 min with the above flow rates. At the end of each sample injection, running buffer was introduced and flowed over the sensor surface for 10 min to enable dissociation. At the end of the dissociation phase, the sensor surface was regenerated for the next sample using 0.1% (w/v) SDS and 0.085% (v/v) H_3PO_4 injected for 1 min at a flow rate of 80 μL/min. For data analysis, sensorgrams were exported from the Biacore T100 Evaluation Software to plot graphs using Origin 8.0 (OriginLab, Northampton). To calculate the K_D, the signal from the reference flow cell containing ethanolamine was subtracted from each value to correct for the contribution of non-specific interactions and systematic errors. Association and dissociation phase data were globally fitted to a simple 1:1 interaction model [$(A + B)$ AB].

Funding

This work was supported by the Max-Planck Society, the Swiss National Science Foundation (SNF grant 205321-107651), the Körber Foundation and the Fondation Bay.

Acknowledgements

We are very grateful to Dr Dziadek from the Department of Immunoparasitology, University of Lodz, Lodz, Poland, for providing us with the plasmids pHis-ROP2 and pHis-ROP4. We would like to gratefully acknowledge Dr V. Mountain for critically editing the manuscript. N.A. thanks B. Monnanda Ponnappa for his help in flow cytometry analyses.

Conflict of interest

None declared.

Abbreviations

AFM, atomic force microscopy; BSA, bovine serum albumin; CS, chondroitin sulfate; DMEM, Dulbecco's modified Eagle's medium; EDTA, ethylenediaminetetraacetic acid; FACS, fluorescence activated cell sorting; FCS, fetal calf serum; GAG, glycosaminoglycan; GFP, green fluorescent protein; GlcN-IdoA, glucosamine-iduronic acid; GRA, granule; HypoS, hyposulfated; K_D, equilibrium dissociation constant; KO, knockout; MALDI-TOF MS, matrix-assisted laser desorption/ionization-time of flight-mass spectrometry; mAb, monoclonal antibody; $NaClO_3$, sodium chlorate; PBS, phosphate-buffered saline; Rec, recombinant; ROP, rhoptry; RT, room temperature; SDS–PAGE, sodium dodecyl sulfate–polyacrylamide gel electrophoresis; SPR, surface plasmon resonance; Vero, African Green Monkey Kidney; wt, wild type.

References

Achur RN, Kakizaki I, Goel S, Kojima K, Madhunapantula SV, Goyal A, Ohta M, Kumar S, Takagaki K, Gowda CD. 2008. Structural interactions in chondroitin 4-sulfate mediated adherence of *Plasmodium falciparum* infected erythrocytes in human placenta during pregnancy-associated malaria. *Biochemistry.* 47:12635–12643.

Adibekian A, Bindschädler P, Timmer MS, Noti C, Schutzenmeister N, Seeberger PH. 2007. De novo synthesis of uronic acid building blocks for assembly of heparin oligosaccharides. *Chemistry.* 13:4510–4522.

Bäckström G, Höök M, Lindahl U, Feingold DS, Malmström A, Rodén L, Jacobsson I. 1979. Biosynthesis of heparin. Assay and properties of the microsomal uronosyl C-5 epimerase. *J Biol Chem*. 254:2975–2982.

Baeuerle PA, Huttner WB. 1986. Chlorate a potent inhibitor of protein sulfation in intact cells. *Biochem Biophys Res Commun*. 141:870–877.

Barragan A, Brossier F, Sibley LD. 2005. Transepithelial migration of *Toxoplasma gondii* involves an interaction of intercellular adhesion molecule 1 (ICAM-1) with the parasite adhesin MIC2. *Cell Microbiol*. 7:561–568.

Baum J, Pinder M, Conway DJ. 2003. Erythrocyte invasion phenotypes of *Plasmodium falciparum* in The Gambia. *Infect Immun*. 71:1856–1863.

Bishop JR, Crawford BE, Esko JD. 2005. Cell surface heparan sulfate promotes replication of *Toxoplasma gondii*. *Infect Immun*. 73:5395–401.

Bitter T, Muir HM. 1962. A modified uronic acid carbazole reaction. *Anal Biochem*. 4:330–434.

Black MW, Boothroyd JC. 2000. Lytic cycle of *Toxoplasma gondii*. *Microbiol Mol Biol*. 64:607–623.

Blader IJ, Saeij JP. 2009. Communication between *Toxoplasma gondii* and its host: Impact on parasite growth, development, immune evasion, and virulence. *APMIS*. 117:458–476.

Blumenschein TMA, Friedrich N, Childs RA, Saouros S, Carpenter EP, Campanero-Rhodes MA, Simpson P, Chai W, Koutroukides T, Blackman MJ, et al. 2007. Atomic resolution insight into host cell recognition by *Toxoplasma gondii*. *EMBO J*. 26:2808–2820.

Botero-Kleiven S, Fernández V, Lindh J, Richter-Dahlfors A, von Euler A, Wahlgren M. 2001. Receptor-mediated endocytosis in an apicomplexan parasite (*Toxoplasma gondii*). *Exp Parasitol*. 98:134–144.

Boulanger MJ, Tonkinan ML, Crawford J. 2010. Apicomplexan parasite adhesins: Novel strategies for targeting host cell carbohydrates. *Curr Opin Struct Biol*. 20:551–559.

Boyle MJ, Richards JS, Gilson PR, Chai W, Beeson JG. 2010. Interactions with heparin-like molecules during erythrocyte invasion by *Plasmodium falciparum* merozoites. *Blood*. 115:4559–4568.

Brenier-Pinchart MP, Villena I, Mercier C, Durand F, Simon J, Cesbron-Delauw MF, Pelloux H. 2006. The *Toxoplasma* surface protein SAG1 triggers efficient *in vitro* secretion of chemokine ligand 2 (CCL2) from human fibroblasts. *Microbes Infect*. 8:254–261.

Brown A, Higgins MK. 2010. Carbohydrate binding molecules in malaria pathology. *Curr Opin Struct Biol*. 20:560–566.

Carruthers V, Boothroyd JC. 2007. Pulling together: An integrated model of *Toxoplasma* cell invasion. *Curr Opin Microbiol*. 10:83–89.

Carruthers VB, Giddings OK, Sibley LD. 1999. Secretion of micronemal proteins is associated with *Toxoplasma* invasion of host cells. *Cell Microbiol*. 1:225–235.

Carruthers VB, Håkansson S, Giddings OK, Sibley LD. 2000. *Toxoplasma gondii* uses sulfated proteoglycans for substrate and host cell attachment. *Infect Immun*. 68:4005–4011.

Carruthers VB, Sibley LD. 1997. Sequential protein secretion from three distinct organelles of *Toxoplasma gondii* accompanies invasion of human fibroblasts. *Eur J Cell Biol*. 73:114–123.

Carruthers VB, Sibley LD. 1999. Mobilization of intracellular calcium stimulates microneme discharge in *Toxoplasma gondii*. *Mol Microbiol*. 31:421–428.

Carruthers VB, Tomley FM. 2008. Microneme proteins in apicomplexans. *Subcell Biochem*. 47:33–45.

Cérède O, Dubremetz JF, Bout D, Lebrun M. 2002. The *Toxoplasma gondii* protein MIC3 requires pro-peptide cleavage and dimerization to function as adhesin. *EMBO J*. 21:2526–2536.

Cesbron-Delauw MF, Boutillon C, Mercier C, Fourmaux MP, Murray A, Miquey F, Tartar A, Capron A. 1992. Amino acid sequence requirements for the epitope recognized by a monoclonal antibody reacting with the secreted antigen GP28.5 of *Toxoplasma gondii*. *Mol Immunol*. 29:1375–1382.

Cesbron-Delauw MF, Gendrin C, Travier L, Ruffiot P, Mercier C. 2008. Apicomplexa in mammalian cells: Trafficking to the parasitophorous vacuole. *Traffic*. 9:657–664.

Charif H, Darcy F, Torpier G, Cesbron-Delauw MF, Capron A. 1990. *Toxoplasma gondii*: Characterization and localization of antigens secreted from tachyzoites. *Exp Parasitol*. 71:114–124.

Coppi A, Tewari R, Bishop JR, Bennett BL, Lawrence R, Esko JD, Billker O, Sinnis P. 2007. Heparan sulfate proteoglycans provide a signal to *Plasmodium* sporozoites to stop migrating and productively invade host cells. *Cell Host Microbe*. 2:316–327.

Couvreur G, Sadak A, Fortier B, Dubremetz JF. 1988. Surface antigens of *Toxoplasma gondii*. *Parasitology*. 97:1–10.

Cowman AF, Crabb BS. 2006. Invasion of red blood cells by malaria parasites. *Cell*. 124:755–766.

de Paz JL, Noti C, Seeberger PH. 2006. Preparation and use of microarrays containing synthetic heparin oligosaccharides for the rapid analysis of heparin-protein interactions. *J Am Chem Soc*. 128:2766–2767.

Doktycz MJ, Sullivan CJ, Hoyt PR, Pelletier DA, Wu S, Allison DP. 2003. AFM imaging of bacteria in liquid media immobilized on gelatin coated mica surfaces. *Ultramicroscopy*. 97:209–216.

Dubremetz JF, Garcia-Réguet M, Conseil V, Fourmaux MN. 1998. Apical organelles and host-cell invasion by Apicomplexa. *Int J Parasitol*. 28:1007–1013.

Dziadek B, Gatkowska J, Brzostek A, Dziadek J, Dzitko K, Dlugonska H. 2009. *Toxoplasma gondii*: The immunogenic and protective efficacy of recombinant ROP2 and ROP4 rhoptry proteins in murine experimental toxoplasmosis. *Exp Parasitol*. 123:81–89.

El Hajj H, Papoin J, Cérède O, Garcia-Réguet N, Soête M, Dubremetz JF, Lebrun M. 2008. Molecular signals in the trafficking of *Toxoplasma gondii* protein MIC3 to the micronemes. *Eukaryot Cell*. 7:1019–1028.

Friedrich N, Matthews S, Soldati-Favre D. 2010. Sialic acids: Key determinants for invasion by the Apicomplexa. *Int J Parasitol*. 40:1145–1154.

Friedrich N, Santos JM, Liu Y, Palma AS, Leon E, Saouros S, Kiso M, Blackman MJ, Matthews S, Feizi T, et al. 2010. Members of a novel protein family containing microneme adhesive repeat domains act as sialic acid-binding lectins during host cell invasion by apicomplexan parasites. *J Biol Chem*. 285:2064–2076.

Garénaux E, Shams-Eldin H, Chirat F, Bieker U, Schmidt J, Michalski JC, Cacan R, Guérardel Y, Schwarz RT. 2008. The dual origin of *Toxoplasma gondii N*-glycans. *Biochemistry*. 47:12270–12276.

Garnett JA, Liu Y, Leon E, Allman SA, Friedrich N, Saouros S, Curry S, Soldati-Favre D, Davis BG, Feizi T, et al. 2009. Detailed insights from microarray and crystallographic studies into carbohydrate recognition by microneme protein 1 (MIC1) of *Toxoplasma gondii*. *Protein Sci*. 18:1935–1947.

Golkar M, Rafati S, Abdel-Latif MS, Brenier-Pinchart MP, Fricker-Hidalgo H, Sima BK, Babaie J, Pelloux H, Cesbron-Delauw MF, Mercier C. 2007. The dense granule protein GRA2, a new marker for the serodiagnosis of acute *Toxoplasma* infection: Comparison of sera collected in both France and Iran from pregnant women. *Diagn Microbiol Infect Dis*. 58:419–426.

Guerrero-Martinez A, Fibikar S, Pastoriza-Santos I, Liz-Marzán LM, De Cola L. 2009. Microcontainers with fluorescent anisotropic zeolite L cores and isotropic silica shells. *Angew Chem Int Ed*. 48:1266–1270.

He XL, Grigg ME, Boothroyd JC, Garcia KC. 2002. Structure of the immunodominant surface antigen from the *Toxoplasma gondii* SRS superfamily. *Nat Struct Biol*. 9:606–611.

Humphries DE, Silbert JE. 1988. Chlorate: A reversible inhibitor of proteoglycan sulfation. *Res Comm*. 154:365–371.

Jacquet A, Coulon L, De Nève J, Daminet V, Haumont M, Garcia L, Bollen A, Jurado M, Biemans R. 2001. The surface antigen SAG3 mediates the attachment of *Toxoplasma gondii* to cell-surface proteoglycans. *Mol Biochem Parasitol*. 116:35–44.

Khil'chenko SR, Zaporozhets TS, Shevchenko NM, Zvyagintseva TN, Vogel U, Seeberger PH, Lepenies B. 2011. Immunostimulatory activity of fucoidan from the Brown Alga *Fucus evanescens*: Role of sulfates and scetates. *J Carb Chem*. 30:291–305.

Kosakai M, Yamauchi F, Yosizawa Z. 1978. Isolation and characterization of sulfated disaccharides from the deamination products of porcine heparin (α-Heparin) and whale heparin (ω-Heparin), and a comparison of the deamination products. *J Biochem*. 83:1567–1575.

Laemmli UK. 1970. Cleavage of structural proteins during the assembly of the head of bacteriophage T4. *Nature*. 227:680–685.

Lee YC, Lee RT. 1995. Carbohydrate-protein interactions: Basis of glycobiology. *Acc Chem Res*. 28:321–327.

Lekutis C, Ferguson DJ, Grigg ME, Camps M, Boothroyd JC. 2001. Surface antigens of *Toxoplasma gondii*: Variations on a theme. *Int J Parasitol*. 31:1285–1292.

Leriche MA, Dubremetz JF. 1991. Characterization of the protein contents of rhoptries and dense granules of *Toxoplasma gondii* tachyzoites by subcellular fractionation and monoclonal antibodies. *Mol Biochem Parasitol*. 45:249–260.

Menard R. 2001. Gliding motility and cell invasion by Apicomplexa: Insights from the *Plasmodium* sporozoite. *Cell Microbiol*. 3:63–73.

Mercier C, Cesbron-Delauw MF, Sibley LD. 1998. The amphipathic alpha helices of the *Toxoplasma* protein GRA2 mediate post-secretory membrane association. *J Cell Sci*. 111:2171–2180.

Mercier C, Lecordier L, Darcy F, Deslée D, Murray A, Tourvieille B, Maes P, Capron A, Cesbron-Delauw MF. 1993. Molecular characterization of a dense granule antigen (GRA2) associated with the network of the parasitophorous vacuole in *Toxoplasma gondii*. *Mol Biochem Parasitol*. 58:71–82.

Mineo JR, McLeod R, Mack D, Smith J, Khan IA, Ely KH, Kasper LH. 1993. Antibodies to *Toxoplasma gondii* major surface protein (SAG-1, P30) inhibit infection of host cells and are produced in murine intestine after peroral infection. *J Immunol*. 150:3951–3964.

Monteiro VG, Soares CP, de Souza W. 1998. Host cell surface sialic acid residues are involved on the process of penetration of *Toxoplasma gondii* into mammalian cells. *FEMS Microbiol Lett*. 164:323–327.

Muthusamy A, Achur RN, Valiyaveettil M, Botti JJ, Taylor DW, Leke RF, Gowda DC. 2007. Chondroitin sulfate proteoglycan but not hyaluronic acid is the receptor for the adherence of *Plasmodium falciparum*-infected erythrocytes in human placenta, and infected red blood cell adherence up-regulates the receptor expression. *Am J Pathol*. 170:1989–2000.

Noti C, de Paz JL, Polito L, Seeberger PH. 2006. Preparation and use of microarrays containing synthetic heparin oligosaccharides for the rapid analysis of heparin-protein interactions. *Chemistry*. 12:8664–8686.

Ortega-Barria E, Boothroyd JC. 1999. A *Toxoplasma* lectin-like activity specific for sulfated polysaccharides is involved in host cell infection. *J Biol Chem*. 274:1267–1276.

Persson KE, McCallum FJ, Reiling L, Lister NA, Stubbs J, Cowman AF, Marsh K, Beeson JG. 2008. Variation in use of erythrocyte invasion pathways by *Plasmodium falciparum* mediates evasion of human inhibitory antibodies. *J Clin Invest*. 118:342–351.

Plattner F, Soldati-Favre D. 2008. Hijacking of host cellular functions by the Apicomplexa. *Annu Rev Microbiol*. 62:471–487.

Sabin AB. 1941. Toxoplasmic encephalitis in children. *J Am Med Assoc*. 116:801–807.

Sadak A, Taghy Z, Fortier B, Dubremetz JF. 1988. Characterization of a family of rhoptry proteins of *Toxoplasma gondii*. *Mol Biochem Parasitol*. 29:203–211.

Saffer LD, Mercereau-Puijalon O, Dubremetz JF, Schwartzman JD. 1992. Localization of a *Toxoplasma gondii* rhoptry protein by immunoelectron microscopy during and after host cell penetration. *Protozool*. 39:526–530.

Soldati D, Dubremetz JF, Lebrun M. 2001. Microneme proteins: Structural and functional requirements to promote adhesion and invasion by the apicomplexan parasite *Toxoplasma gondii*. *Int J Parasitol*. 31:1293–1302.

Soldati D, Foth BJ, Cowman AF. 2004. Molecular and functional aspects of parasite invasion. *Trends Parasitol*. 20:567–574.

Soldati-Favre D. 2008. Molecular dissection of host cell invasion by the apicomplexans: The glideosome. *Parasite*. 15:197–205.

Strassert CA, Otter M, Albuquerque RQ, Höne A, Vida Y, Maier B, De Cola L. 2008. Photoactive hybrid nanomaterial for targeting, labeling, and killing antibiotic-resistant bacteria. *Angew Chem Int Ed*. 42:7928–7931.

Thompson JK, Triglia T, Reed MB, Cowman AF. 2001. A novel ligand from *Plasmodium falciparum* that binds to a sialic acid-containing receptor on the surface of human erythrocytes. *Mol Microbiol*. 41:47–58.

Travier L, Mondragon R, Dubremetz JF, Musset K, Mondragon M, Gonzalez S, Cesbron-Delauw MF, Mercier C. 2008. Functional domains of the *Toxoplasma* GRA2 protein in the formation of the membranous nanotubular network of the parasitophorous vacuole. *Int J Parasitol*. 38:757–773.

Triglia T, Duraisingh MT, Good RT, Cowman AF. 2005. Reticulocyte-binding protein homologue 1 is required for sialic acid-dependent invasion into human erythrocytes by *Plasmodium falciparum*. *Mol Microbiol*. 55:162–174.

Varki A. 1997. Sialic acids as ligands in recognition phenomena. *FASEB J*. 11:248–255.

Varki A. 2008. Sialic acids in human health and disease. *Trends Mol Med*. 14:351–360.

Velge-Roussel F, Dimier-Poisson I, Buzoni-Gatel D, Bout D. 2001. Anti-SAG1 peptide antibodies inhibit the penetration of *Toxoplasma gondii* tachyzoites into enterocyte cell lines. *Parasitology*. 123:225–233.

Vogt AM, Barragan A, Chen Q, Kironde F, Spillmann D, Wahlgren M. 2003. Heparan sulfate on endothelial cells mediates the binding of *Plasmodium falciparum*-infected erythrocytes via the DBL1alpha domain of PfEMP1. *Blood*. 101:2405–2411.

Zinecker CF, Striepen B, Geyer H, Geyer R, Dubremetz JF, Schwarz RT. 2001. Two glycoforms are present in the GPI-membrane anchor of the surface antigen 1 (P30) of *Toxoplasma gondii*. *Mol Biochem Parasitol*. 116:127–135.